Primary clear-cell carcinoma of the liver with gastric antrum metastasis: Integrated management with targeted therapy, immunotherapy and salvage surgery: A case report

LIANSHAN ZHAN[1], QIANWEI LI[1], TIAN TIAN[1] and LONG WANG[2]

[1]Department of Nuclear Medicine, Guiqian International Hospital, Guiyang, Guizhou 551008, P.R. China;
[2]Department of Pathology, Guiqian International Hospital, Guiyang, Guizhou 551008, P.R. China

Received September 2, 2025; Accepted February 9, 2026

DOI: 10.3892/ol.2026.15516

Abstract. This study reports the case of a patient diagnosed with primary clear-cell carcinoma of the liver (PCCCL). Intrahepatic metastasis transpired 1 month subsequent to the resection of the intrahepatic primary lesion. Subsequently, the patient commenced systemic treatment utilizing a combination of targeted drugs and programmed cell death-1 inhibitor. Immune-related adverse events (irAEs) manifested during the treatment process, encompassing persistent myelosuppression, hypothyroidism and a substantial elevation of adrenocorticotropic hormone levels. Rare gastric metastasis was identified during the follow-up course. Through multidisciplinary collaboration, entailing the sequential or combined implementation of surgery, targeted therapy and immunotherapy, along with the effective management of irAEs, the primary tumor, intrahepatic metastases and gastric metastasis in the patient were all effectively controlled. At the final follow-up, no signs of recurrence or metastasis were observed. This case underscores the highly invasive attributes of PCCCL, the diverse metastatic modalities (particularly the rare gastric metastasis), the actual efficacy of systemic treatment and the importance of complex irAE management, thus offering key guidelines for clinical practice.

Introduction

Primary clear-cell carcinoma of the liver (PCCCL) is an infrequent subtype of hepatocellular carcinoma (HCC), with its incidence constituting 3-7% of all cases of HCC. Pathologically, >50% of the tumor cells display clear cytoplasm replete with glycogen. In comparison with common HCC, certain reports propose that PCCCL may possess relatively lower invasiveness and a more favorable prognosis. However, other investigations have indicated that it is predisposed to microvascular invasion (MVI) and extra-hepatic metastasis (1). As a result, the overall survival outcome of PCCCL remains a subject of contention.

While clear cell morphology can also occur in metastatic renal cell carcinoma and other primary hepatic neoplasms, immunohistochemical (IHC) confirmation of hepatocellular origin using markers such as hepatocyte paraffin antigen 1 (HepPar-1), arginase-1 (Arg-1) and glypican-3 (GPC3) becomes essential for the accurate diagnosis of PCCCL (2,3). Furthermore, recent genomic studies have revealed that PCCCL may harbor distinct molecular alterations compared with conventional HCC, including a lower frequency of tumor protein 53 mutations and enrichment of catenin β1 mutations, which could partially explain its relatively indolent behavior in a subset of patients (4).

Currently, the treatment of advanced PCCCL primarily adheres to the HCC diagnosis and treatment guidelines, with surgical intervention serving as the cornerstone of treatment. The combination of targeted therapy and immune checkpoint inhibitors, such as programmed cell death (PD)-1 monoclonal antibodies, is assuming an increasingly prominent role (5). Nevertheless, there is still a substantial dearth of data regarding the differential efficacy of this subtype in systemic treatment and its long-term survival rates. The present case report aims to augment the diagnostic and therapeutic approaches and experiences of PCCCL in clinical practice.

Case report

A 37-year-old female patient was admitted to the hospital in October 2021, presenting with persistent distending pain in the right upper abdomen for 15 days. Throughout the disease course, the patient did not exhibit any symptoms such as nausea, vomiting, anorexia, fatigue, fever, chills or jaundice. The past medical, family and personal history of the patient was unremarkable. Upon admission, a series of laboratory examinations were carried out (normal reference values are provided in parentheses): Alanine aminotransferase was 27.7 U/l (7.0-40.0 U/l), aspartate aminotransferase was 21.5 U/l (13.0-35.0 U/l) and total bilirubin was 9.0 μmol/l

Correspondence to: Professor Lianshan Zhan, Department of Nuclear Medicine, Guiqian International Hospital, 1 Dongfeng Avenue, Wudang, Guiyang, Guizhou 551008, P.R. China
E-mail: zhanlianshan1988@126.com

Key words: primary clear-cell carcinoma of the liver, gastric metastasis, immune-related adverse events, systemic therapy

(5.0-21.0 μmol/l). The results of the hepatitis B serological profile were as follows: Hepatitis B surface antigen (HBsAg), <0.1 index (<1 index); antibody to hepatitis B surface antigen, 17.9 mIU/ml (<8.0 mIU/ml); hepatitis Be antigen, 0 index (<0.8 index); hepatitis Be antibody, 0.2 index (<0.8 index) and hepatitis B core antibody, 0.1 index (<0.5 index). The α-fetoprotein (AFP) level was 33.9 ng/ml (<25.0 ng/ml), and no elevation was detected in carcinoembryonic antigen, ferritin or carbohydrate antigen 19-9. Abdominal computed tomography (CT) revealed that the liver maintained its normal shape and size. However, an irregular mixed-density mass (containing fat density; Fig. 1A) was identified in segment S6 of the liver. In October 2021, the patient underwent resection of this segment S6. During the operation, the liver was found to be of normal size, with a soft texture and a healthy red color. The exophytic mass in segment S6 of the liver was densely adherent to the omentum of the hepatic flexure of the colon. The tumor had two areas of rupture, accompanied by tiny nodules in the adjacent omentum. Postoperative pathological examination indicated clear cell carcinoma in segment S6 of the liver. In >50% of the tumor cells, clear cytoplasm was observed, which was rich in glycogen (Fig. 1E). According to the Edmondson-Steiner grading system, the mass was classified as grade III. MVI was present (MVI grading, M2), and cancer metastasis was evident in the omental nodules. IHC analysis showed positive results for hepatocyte (Fig. 1F), GPC3 (Fig. 1G) and Ki-67 (40% positive) (Fig. 1H). The postoperative diagnosis was PCCCL (Clinical Research Group of Liver Cancer stage IIIa).

In November 2021, prior to planned further systemic treatment, a follow-up abdominal MRI showed a newly detected subcapsular nodule (18x10 mm) in segmen 7 (S7) of the liver. On T1-weighted imaging, it presented as a slightly hypointense signal lesion (Fig. 2A). Contrast-enhanced scanning showed mild heterogeneous enhancement, and there was no contrast agent uptake during the hepatobiliary-specific phase, which was diagnosed as intrahepatic metastasis (Fig. 2B-D). Subsequently, the patient was administered a combination therapy of lenvatinib (8 mg once daily) and toripalimab (240 mg).

Following the completion of six cycles of immunotherapy, an abdominal CT in July 2022 revealed that the nodule in the liver had not notably diminished in size (17.0x11.0 mm). The treatment regimen was adjusted to lenvatinib at 8 mg once daily in combination with tislelizumab at 200.0 mg every 3 weeks for maintenance treatment. Endoscopy examination indicated antral gastritis and inflammatory alterations in the terminal ileum and the colon. Persistent myelosuppression was noted, with a white blood cell count of $3.3x10^9$/l. Thyroid function was abnormal, with the following specific parameters: Thyroid stimulating hormone, 22.6 mIU/l (0.5-4.7 mIU/l); FT3 and FT4 were normal. The adrenocorticotropic hormone (ACTH) level was 32.4 pg/ml (1.6-13.9 pg/ml between 7:00 and 10:00 a.m.). The patient was regularly followed up in the outpatient clinic during this period and continued to receive combination therapy with lenvatinib and tislelizumab. In August 2023, laboratory results revealed an ACTH concentration of 816.0 pg/ml, the patient experienced an immune-related adverse event (irAEs). As a result, immunotherapy was temporarily suspended. An abdominal CT scan 2 months later indicated that the nodule in the liver had regressed to 10.0x9.0 mm. A laparoscopic resection of liver S7 was performed. The pathological report suggested that the nodule exhibited necrosis subsequent to the treatment for HCC. A postoperative ACTH level of 69.8 pg/ml confirmed the condition and maintenance therapy with lenvatinib combined with tislelizumab was continued.

In June 2024, the patient was admitted to the same hospital presenting with 'melena accompanied by dizziness, fatigue and transient aphasia'. Blood routine examination results showed a hemoglobin level of 70.0 g/l (115.0-170.0 g/l) and the fecal occult blood test was positive. Gastroscopy revealed a 2.5-cm submucosal elevation at the greater curvature of the gastric antrum, with ulceration and bleeding at the apex (Fig. 3A). Abdominal CT showed thickening of the gastric antrum wall ≤21.0 mm. ^{18}F-fluorodeoxyglucose (^{18}F-FDG) positron emission tomography/CT (PET/CT) imaging indicated increased ^{18}F-FDG uptake of the gastric antrum mass (Fig. 3B); no other abnormalities were detected throughout the body. After blood transfusion and acid-suppressing and gastric-protecting therapies, the symptoms of the patient were alleviated. In July 2024, the patient underwent a distal gastrectomy with gastrojejunostomy. Based on gastroscopy findings, ^{18}F-FDG PET/CT imaging results and pathological analysis of the gastric antral tumor (Fig. 3), the final diagnosis was metastatic hepatocellular carcinoma. The tumor was located in the whole layer of the gastric wall, without penetration of the serosa layer and the resection margins were negative. IHC analysis showed hepatocyte (-) (Fig. 3C), Arg-1 (+) (Fig. 3D) and GPC3 (+) (Fig. 3E). All tissue samples were fixed in 4% formaldehyde, embedded in paraffin and sectioned. Histological assessment: Tissue samples were fixed in 4% formaldehyde at room temperature for 24 h, then embedded in paraffin. Sections of 4 μm thickness were cut and stained with H&E according to standard protocols. Briefly, sections were deparaffinized, rehydrated, stained with hematoxylin for 5 min at room temperature, washed, stained with eosin for 2 min at room temperature, dehydrated, and mounted. Images were captured using a light microscope (BX53; Olympus Corp.) at x200 magnification; scale bars are indicated in the figure legends.

IHC analysis: IHC was performed on 4-μm paraffin sections using a Roche Ventana Benchmark XT automated staining system (Roche Diagnostics) following the manufacturer's instructions. The staining protocol included deparaffinization, antigen retrieval (CCI solution; Roche Diagnostics) and blocking of endogenous peroxidase. Sections were incubated with primary antibodies against HepPar-1 (cat. no. ZM-0133; 1:100 dilution), GPC3 (cat. no. ZM-0356; 1:200 dilution), Arg-1 (cat. no. ZM-0235; 1:200 dilution) and Ki-67 (ZM-0166; 1:150 dilution). All antibodies were obtained from Shanghai Zhongshan Jinqiao Biotechnology Co., Ltd. All primary antibodies were incubated at 37°C for 32 min. Detection was performed using the UltraView Universal DAB Detection Kit (Roche Diagnostics) according to the manufacturer's protocol, which includes a secondary antibody (goat anti-mouse/rabbit IgG conjugated with horseradish peroxidase). The sections were counterstained with hematoxylin, dehydrated and

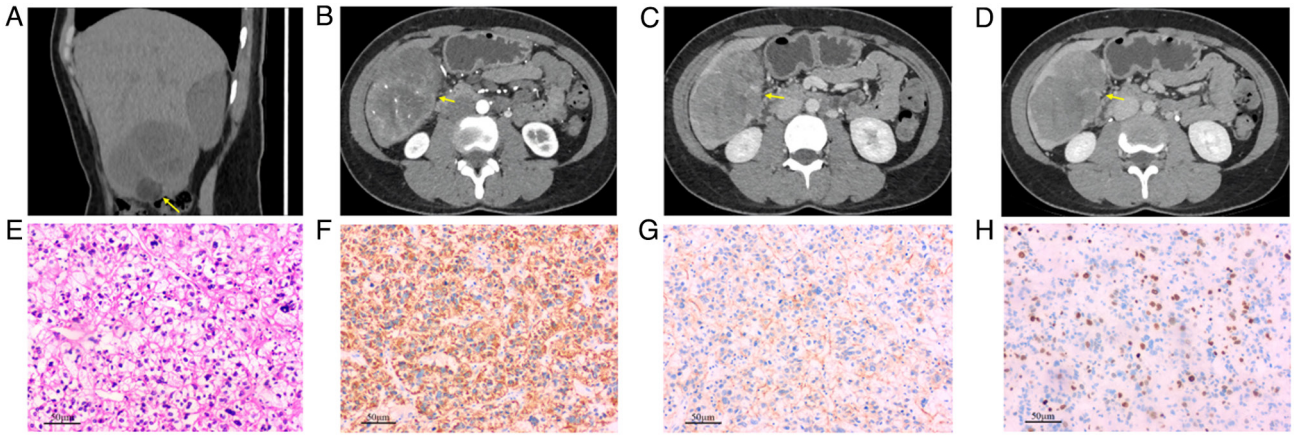

Figure 1. (A) Preoperative non-contrast CT revealed an irregular, mixed-density mass situated in segment S6 (as indicated by the yellow arrow in the figure, the same applies to B-D), which contained fat components. The mass measured 7.31x4.92 cm, with CT values ranging from -11 to 34 HU. (B) During the arterial phase of CT enhancement scanning, multiple small vessels traverse the tumor, demonstrating moderate heterogeneous enhancement. (C) In the venous phase and (D) the delayed phase, the degree of enhancement diminishes, manifesting as the characteristic of 'fast-in and fast-out'. (E) H&E staining revealed that the tumor tissue was predominantly constituted by a high proportion (80%) of vacuolated clear cells. The tumor cells were arranged in a sheet-like or nested configuration and exhibited a large cell volume. The cytoplasm appeared transparent and vacuolated, whereas the nuclei demonstrated irregular morphologies, suggesting marked nuclear atypia. Notably, mitotic figures were rarely observed (scale bar, 50 μm). (F-H) Immunohistochemistry: (F) Hepatocyte (+), (G) glypican-3 (-) and (H) Ki-67 40% (scale bar, 50 μm).

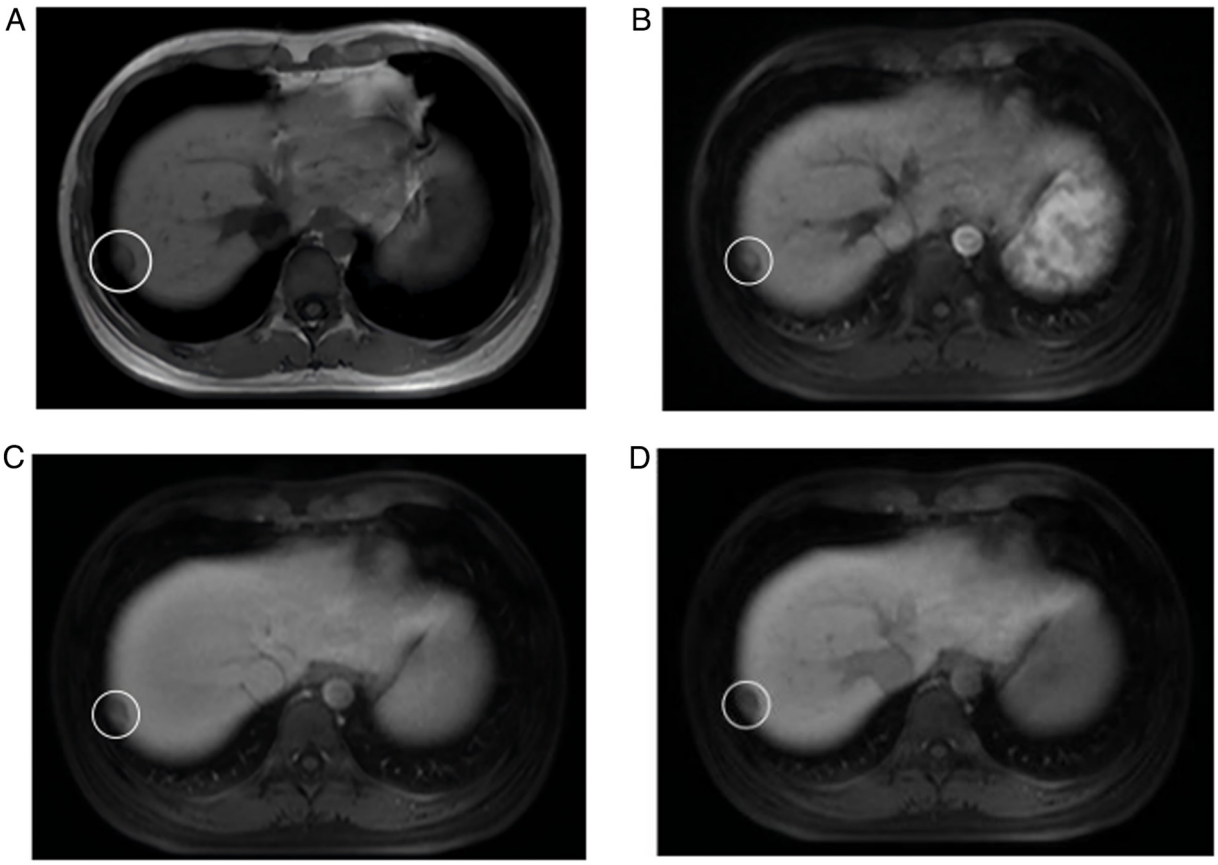

Figure 2. At 1 month after resection of the primary tumor of liver segment S6, MRI findings were as follows: (A) As shown by the white circle, the hepatic nodule in segment 7 presents with a slightly hypointense signal on T1-weighted imaging and an annular hypointense capsule is observable. (B) In the arterial phase of contrast-enhanced scanning, the lesion manifests with mild heterogeneous enhancement without capsular enhancement. In the (C) portal venous and (D) delayed phase, the extent of enhancement diminishes.

mounted. Appropriate positive and negative controls were included. Images were captured with a light microscope (Olympus BX53) at x200 magnification.

After 2 months of recovery, the patient was switched to the second-line treatment for liver cancer: Apatinib 750 mg once a day, combined with tislelizumab. As of the last follow-up

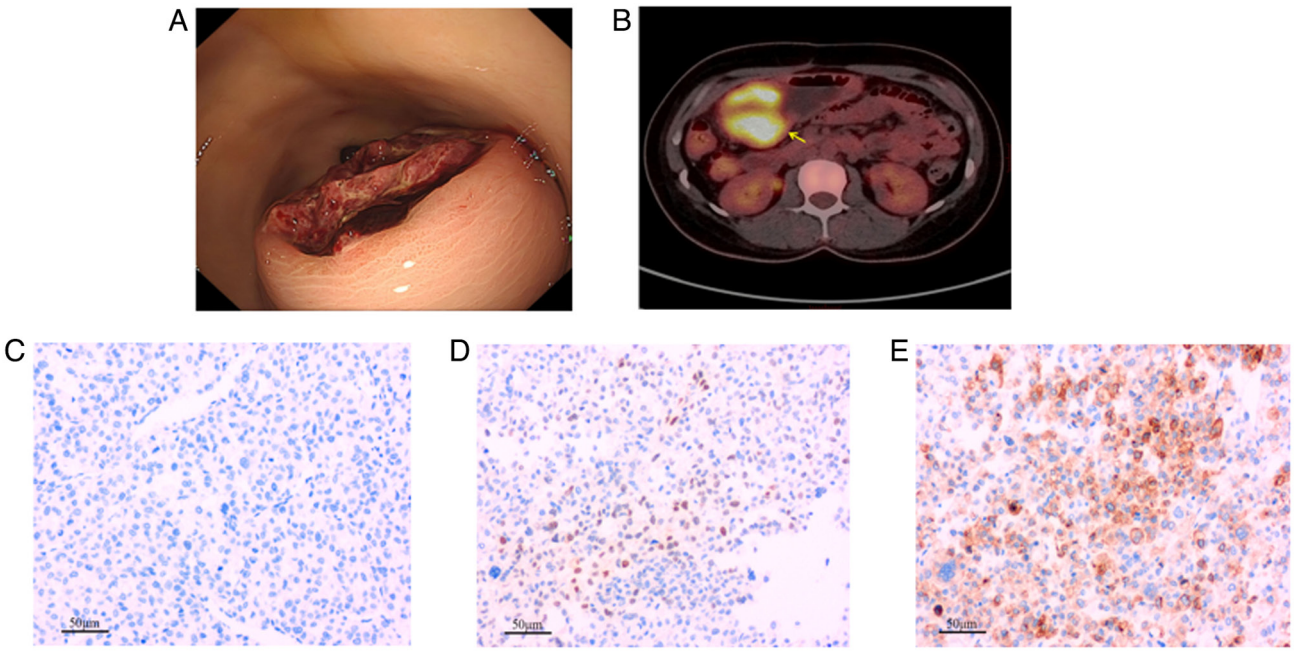

Figure 3. Non-continuous lenvatinib combined with tislelizumab after 23 months of treatment. (A) Gastroscopic examination reveals a submucosal elevated lesion, measuring 2.5 cm on the anterior wall of the gastric antrum. The surface of the lesion is irregular, with localized areas covered by a small quantity of white exudate and dark-red blood clots. (B) ^{18}F-FDG PET/CT imaging indicates increased FDG uptake within the lesion, with a maximum standardized uptake volume of 11.3 (yellow arrow). (C-E) Immunohistochemistry: (C) Hepatocyte (-), (D) Arg-1 (+) and (E) glypican- 3 (+) (scale bars, 50 μm). FDG, fluorodeoxyglucose.

in July 2025, there was no evidence indicating recurrence or metastasis.

Discussion

There are no significant differences in age, sex, preoperative AFP level, liver cirrhosis and clinical symptoms between patients with PCCCL and those with common HCC (CHCC) (6). However, the incidence of hepatitis C infection in patients with PCCCL is higher compared with that of patients with CHCC. The clinical diagnosis mainly relies on pathological examination: The cancer cells of PCCCL are characterized by cytoplasm rich in glycogen or fat, a decrease in the number and volume of organelles and mild nuclear atypia. Histological examination reveals a moderate degree of differentiation (7). Therefore, some literature reports indicate that the prognosis of this disease is generally favorable compared with that of CHCC (8). Although rare, gastric metastasis of HCC has been previously documented in the literature (9).

The contrast-enhanced CT images of the lesion in the present case report demonstrate moderate heterogeneous enhancement during the arterial phase, accompanied by multiple small arteries traversing the lesion. In the venous and delayed phases, the enhancement diminishes, presenting a typical 'fast in, fast out' enhancement pattern similar to that of CHCC. However, CHCC typically exhibits less and milder fatty degeneration. Additionally, the relatively distinct mass boundary and pseudocapsule shadow differ from the infiltrative growth and indistinct boundaries commonly observed in CHCC of the same size or grade (10). PET/CT has limited sensitivity in the initial diagnosis of HCC. Notably, ^{18}F-FDG PET/CT does not offer superior detection efficiency for small intrahepatic metastases compared to contrast-enhanced MRI. Therefore, ^{18}F-FDG PET/CT was not performed prior to the initial surgery. During the histological section examination, it was found that clear cells accounted for >50%. Furthermore, immunohistochemistry results indicated that both the liver-specific antigens hepatocyte and glypican-3 were positive. Considering the absence of abnormalities in other organs detected by imaging, the final diagnosis was confirmed as PCCCL. During the advanced stage of the tumor, the clinical symptoms of the patient lacked specificity. However, the lesion pattern observed by gastroscopy is different from the typical ulcerative or infiltrative growth patterns of primary gastric cancer. By contrast, on enhanced CT scans, the enhancement degree of the gastric antrum lesions was relatively lower compared with that of the primary liver lesions and there was no fat component. This reflected the fundamental difference in tumor cell growth in different microenvironments. To the best of our knowledge, at present, the mechanisms of gastric metastasis of PCCCL remain to be elucidated. It is speculated that renal clear cell carcinoma, which often has distant metastases, may be associated with the abundance of tumor cells, feeding arteries and MVI. Arg-1 exhibits high specificity for HCC; its positivity in the metastasis would strongly confirm a hepatic origin (2). Glypican-3 was focally positive in the gastric metastases, which supported the hepatocyte origin (3). Secondly, hepatocyte (+) in the primary lesion suggests improved differentiation of hepatocytes, while hepatocyte (-) in the metastatic lesion may indicate that the degree of differentiation of metastatic tumor cells had decreased or that they had dedifferentiated, and certain liver phenotypes had been lost (11). This corresponds to the features of the metastatic lesion on ^{18}F-FDG PET/CT imaging (SUVmax=11.3) (12).

As of present, the treatment protocol for PCCCL remains grounded in the general treatment principles of HCC. The patient demonstrated a stable overall health status, with all liver function indices falling within the normal range. Integrating the findings of preoperative imaging examinations, radical resection was identified as the most suitable treatment approach. For the subsequent two surgeries, both the timing and methodology were strictly aligned with current treatment principles. For resectable lesions, including the primary tumor, intrahepatic recurrence foci and symptomatic solitary gastric metastases, proactive surgical intervention is pivotal in controlling local lesions and attaining survival benefits (13). In recent years, clinical investigations into targeted therapy, immunotherapy (both as monotherapy and combination regimens) for advanced HCC have yielded promising results regarding efficacy and safety profiles, thereby informing the selection of first-line therapeutic strategies. For instance, the REFLECT trial demonstrated that lenvatinib was non-inferior to sorafenib in terms of overall survival (OS) among patients with advanced HCC, solidifying the role of lenvatinib as a first-line treatment option for this patient population (14). A separate retrospective study further indicated that the combination of toripalimab, lenvatinib and hepatic artery infusion chemotherapy markedly improved progression-free survival, OS and tumor response rates when compared with lenvatinib monotherapy in the management of advanced HCC (15). Consequently, the patient in the present case report was administered the potent combination regimen of lenvatinib plus a PD-1 inhibitor, which aligns with the recommendations outlined in clinical practice guidelines. However, following the completion of six treatment cycles, CT evaluation revealed no notable reduction in the metastatic lesion located in S7 of the liver. In contrast with toripalimab, tislelizumab features structural modifications to its Fc region, which mitigate macrophage-mediated T-cell exhaustion and theoretically enhance anti-tumor immune responses (16). As evidenced by subsequent imaging studies, switching to the combination therapy of tislelizumab and lenvatinib resulted in a reduction in the liver S7 lesion, thereby facilitating subsequent surgical intervention. Nevertheless, the patient experienced exacerbation of irAEs, necessitating the temporary suspension of immunotherapy. After a 3-month interval during which the irAEs subsided, the first-line treatment regimen was reinitiated.

Given the heterogeneity of HCC, tumor progression frequently ensues following first-line systemic therapy. The low incidence of PCCCL has also constrained the clinical synthesis of therapeutic strategies for PCCCL metastasis. The phenomenon of 'hyperprogressive disease' was first defined in 2017 by Champiat *et al* (17). It refers to disease progression that meets the Response Evaluation Criteria in Solid Tumors at the first imaging evaluation, along with at least a two-fold increase in the tumor growth rate. This phenomenon may be associated with various factors, including specific genetic alterations and immune microenvironment dysregulation. In the present case, however, a young female patient developed gastric antral metastasis 8 months after resuming immunotherapy following a 3-month treatment pause. It is reasonable to consider this progression part of the natural disease course. Apatinib exhibits high specificity for VEGFR-2 binding without antagonizing VEGFR-3, thereby failing to impede the activation of T cells stimulated by immune checkpoint inhibitors and preserving the lymphoid-immune system. Apatinib has been approved for patients with HCC who have experienced failure of or intolerance to at least one prior line of systemic antineoplastic therapy (18). Subsequent to the re-failure of PD-1 inhibitor therapy, the patient demonstrated a favorable response to the combination regimen of apatinib and tislelizumab, with no evidence of tumor recurrence observed during follow-up to the present date.

Acknowledgements

Not applicable.

Funding

No funding was received.

Availability of data and materials

The data generated in the present study may be requested from the corresponding author.

Authors' contributions

LZ contributed to the acquisition and analysis of data, was primarily responsible for collecting the patient's complete clinical data, including imaging, pathology, and follow-up records, participated in the interpretation of data regarding the treatment response and outcome and drafted the initial version of the case report and methods sections of the manuscript. TT contributed to the conception and design of this case study, contributed to the analysis and interpretation of the pathological findings, particularly regarding the rare diagnosis of primary clear-cell carcinoma and critically revised the manuscript for important intellectual content, specifically the discussion section. QL and LW conceived the concept of the article and critically revised the manuscript. LZ and QL confirm the authenticity of all raw data. All authors have read and agreed to the published version of the manuscript.

Ethics approval and consent to participate

Not applicable.

Patient consent for publication

The patient provided written informed consent for the publication of her case details, including clinical data and images.

Competing interests

The authors declare that they have no competing interests.

References

1. Dudani S, de Velasco G, Wells JC, Gan CL, Donskov F, Porta C, Fraccon A, Pasini F, Lee JL, Hansen A, *et al*: Evaluation of clear cell, papillary, and chromophobe renal cell carcinoma metastasis sites and association with survival. JAMA Netw Open 4: e2021869, 2021.

2. Yan BC, Gong C, Song J, Krausz T, Tretiakova M, Hyjek E, Al-Ahmadie H, Alves V, Xiao SY, Anders RA and Hart JA: Arginase-1: A new immunohistochemical marker of hepatocytes and hepatocellular neoplasms. Am J Surg Pathol 34: 1147-1154, 2010.
3. Ligato S, Mandich D and Cartun RW: Utility of glypican-3 in differentiating hepatocellular carcinoma from other primary and metastatic lesions in FNA of the liver: an immunocytochemical study. Mod Pathol 21: 626-631, 2008.
4. Calderaro J, Couchy G, Imbeaud S, Amaddeo G, Letouzé E, Blanc JF, Laurent C, Hajji Y, Azoulay D, Bioulac-Sage P, *et al*: Histological subtypes of hepatocellular carcinoma are related to gene mutations and molecular tumour classification. J Hepatol 67: 727-738, 2017.
5. Donne R and Lujambio A: The liver cancer immune microenvironment: Therapeutic implications for hepatocellular carcinoma. Hepatology 77: 1773-1796, 2023.
6. Liu B, Li J, Yang X, Chen F, Zhang Y and Li H: Diagnosis of primary clear cell carcinoma of the liver based on Faster region-based convolutional neural network. Chin Med J (Engl) 136: 2706-2711, 2023.
7. Liu Z, Ma W, Li H and Li Q: Clinicopathological and prognostic features of primary clear cell carcinoma of the liver. Hepatol Res 38: 291-299, 2008.
8. Li ZY, Bi XY, Zhao JJ, Zhao H, Zhou JG, Huang Z, Cai JQ and Zheng XC: Clinicopathological and prognostic analysis of primary clear cell carcinoma of the liver. Zhonghua Zhong Liu Za Zhi (Chinese) 35: 140-143, 2013.
9. Chen WT, Huang SK, Chang ML and Liaw YF: Hepatocellular carcinoma with gastric metastasis mimicking a 4 cm gastrointestinal stromal tumor after a 3-year disease-free interval. J Clin Transl Hepatol 12: 218-221, 2024.
10. Wang H, Tan B, Zhao B, Gong G and Xu Z: CT findings of primary clear cell carcinoma of liver: With analysis of 19 cases and review of the literature. Abdom Imaging 39: 736-743, 2014.
11. Hanif R and Mansoor S: Hep par-1: A novel immunohistochemical marker for differentiating hepatocellular carcinoma from metastatic carcinoma. J Coll Physicians Surg Pak 24: 186-189, 2014.
12. Yao Y, Civelek AC and Li XF: The application of 18F-FDG PET/CT imaging for human hepatocellular carcinoma: A narrative review. Quant Imaging Med Surg 13: 6268-6279, 2023.
13. Yang X, Yang C, Zhang S, Geng H, Zhu AX, Bernards R, Qin W, Fan J, Wang C and Gao Q: Precision treatment in advanced hepatocellular carcinoma. Cancer Cell 42: 180-197, 2024.
14. Kudo M, Finn RS, Qin S, Han KH, Ikeda K, Piscaglia F, Baron A, Park JW, Han G, Jassem J, *et al*: Lenvatinib versus sorafenib in first-line treatment of patients with unresectable hepatocellular carcinoma: A randomised phase 3 non-inferiority trial. Lancet 391: 1163-1173, 2018.
15. Li Y, Wang D, Zhang F, Zheng X, Song Y, Ran Y and Cai X: Hepatic arterial infusion chemotherapy combined with lenvatinib and toripalimab for large hepatocellular carcinoma (>10 cm) with major portal vein tumor thrombosis: A multicenter propensity score matching analysis. Front Immunol 16: 1638173, 2025.
16. Zhang T, Song X, Xu L, Ma J, Zhang Y, Gong W, Zhang Y, Zhou X, Wang Z, Wang Y, *et al*: The binding of an anti-PD-1 antibody to FcγRI has a profound impact on its biological functions. Cancer Immunol Immunother 67: 1079-1090, 2018.
17. Champiat S, Dercle L, Ammari S, Massard C, Hollebecque A, Postel-Vinay S, Chaput N, Eggermont A, Marabelle A, Soria JC and Ferté C: Hyperprogressive disease is a new pattern of progression in cancer patients treated by anti-PD-1/PD-L1. Clin Cancer Res 23: 1920-1928, 2017.
18. Yu J, Yu J, Chen Y, Yang Y and Yi P: PD-1 inhibitors improve the efficacy of transcatheter arterial chemoembolization combined with apatinib in advanced hepatocellular carcinoma: A meta-analysis and trial sequential analysis. BMC Cancer 25: 564, 2025.